Evolution of the Fermi Surface of $BaFe_2(As_{1-x}P_x)_2$ on Entering the Superconducting Dome

H. Shishido,[1,2] A. F. Bangura,[3] A. I. Coldea,[3] S. Tonegawa,[1] K. Hashimoto,[1] S. Kasahara,[2] P. M. C. Rourke,[3] H. Ikeda,[1] T. Terashima,[2] R. Settai,[4] Y. Ōnuki,[4] D. Vignolles,[5] C. Proust,[5] B. Vignolle,[5] A. McCollam,[6] Y. Matsuda,[1] T. Shibauchi,[1] and A. Carrington[3]

[1]*Department of Physics, Kyoto University, Sakyo-ku, Kyoto 606-8502, Japan*
[2]*Research Center for Low Temperature and Materials Sciences, Kyoto University, Sakyo-ku, Kyoto 606-8501, Japan*
[3]*H. H. Wills Physics Laboratory, Bristol University, Tyndall Avenue, BS8 1TL, United Kingdom*
[4]*Graduate School of Science, Osaka University, Toyonaka, Osaka 560-0043, Japan*
[5]*Laboratoire National des Champs Magnétiques Intenses (CNRS), Toulouse, France*
[6]*High Field Magnet Laboratory, Institute for Molecules and Materials, Radboud University Nijmegen, Toernooiveld 7, 6525 ED Nijmegen, The Netherlands*

(Received 20 October 2009; published 5 February 2010)

Using the de Haas–van Alphen effect we have measured the evolution of the Fermi surface of $BaFe_2(As_{1-x}P_x)_2$ as a function of isoelectric substitution (As/P) for $0.41 < x < 1$ (T_c up to 25 K). We find that the volumes of electron and hole Fermi surfaces shrink linearly with decreasing x. This shrinking is accompanied by a strong increase in the quasiparticle effective mass as x is tuned toward the maximum T_c. These results are not explained by simple band structure calculations, and it is likely that these trends originate from the same many-body interactions which give rise to superconductivity.

DOI: 10.1103/PhysRevLett.104.057008 PACS numbers: 74.70.−b, 71.18.+y, 74.25.Jb

Superconductivity in the 122 iron-pnictide family XFe_2As_2 (where X = Ba, Sr or Ca), can be induced by a variety of means, including doping [1,2], pressure [3] or isoelectric substitution either on the Fe [4] or As sites [5]. The highest T_c achievable by each of these routes is roughly the same. It has been suggested [6–8] that the interband coupling between the hole and electron sheets plays an important role in determining the magnetic or superconducting order formed at low temperature. Discovering how the Fermi surface evolves as a function of the various material parameters which drive the material from an antiferromagnetic spin density wave state, through the superconducting dome and eventually towards a paramagnetic nonsuperconducting metal, should therefore be an important step toward gaining a complete understanding of the mechanism that drives high temperature superconductivity in these materials.

In the antiferromagnetic state it is expected that the Fermi surface suffers a major reconstruction. This is supported experimentally by the observation [9–11] of very low frequency quantum oscillations in the undoped XFe_2As_2 compounds, corresponding to very small Fermi surface pockets which are 1%–2% of the total Brillouin zone planar area. At the other extreme of the phase diagram, where the materials are paramagnetic and nonsuperconducting, quantum oscillation measurements of $SrFe_2P_2$ [12] and $CaFe_2P_2$ [13] show that the Fermi surface is in good agreement with conventional band structure calculations. Up to now, tracking the changes in the Fermi surface across the phase diagram using quantum oscillations has not been possible because of the additional disorder and high H_{c2} introduced by doping. Measurements on the low T_c (6 K) superconducting iron-pnictide LaFePO [14,15] established that the Fermi surface is in broad agreement with band structure with moderate correlation enhancements of the effective mass. It is not clear whether the higher T_c pnictide superconductors, which unlike LaFePO occur in close proximity to a magnetic phase, are also well described by band structure and whether the electronic correlations change significantly.

The substitution of P for As in the series $BaFe_2(As_{1-x}P_x)_2$ offers an elegant way to suppress magnetism and induce superconductivity without doping [16]. As P and As are isovalent, there is no net change in the ratio of electrons to holes and the system remains compensated for all values of x (equal volumes for the electron and hole Fermi surfaces). This series has several remarkable properties which are similar to those observed in cuprate superconductors. First, the temperature dependence of the resistivity changes from a quadratic ($\rho \sim T^2$) to linear behavior ($\rho \sim T$) as the system evolves from a conventional Fermi liquid ($x = 1$) towards the maximum T_c ($x = 0.33$). Second, there is strong evidence from magnetic penetration depth [17], thermal conductivity [17] and NMR [18] measurements that for $x = 0.33$ the superconducting gap has line nodes.

In this Letter, we report the observation of quantum oscillation signals in samples of $BaFe_2(As_{1-x}P_x)_2$ as x is varied across the superconducting dome from $x = 1$ to $x = 0.41$ with $T_c \sim 25$ K ($\simeq 0.8T_c^{\max}$). Our data show that the Fermi surface shrinks and the quasiparticles become heavier as the material is tuned toward the magnetic order phase boundary, at which T_c reaches its maximum.

Single crystal samples of $BaFe_2(As_{1-x}P_x)_2$ were grown as described in Ref. [16]. The x values were determined by an energy dispersive x-ray analyzer. Measurements of the

quantum oscillations in magnetic torque [the de Haas–van Alphen (dHvA) effect] were made using a miniature piezoresistive cantilever technique. Experiments were performed in: a dilution refrigerator system with dc fields up to 17 T (Osaka), a pumped ^{3}He system with dc fields up to 30 T (Nijmegen) and 45 T (Tallahassee) and a pumped ^{4}He system with pulsed fields up to 55 T (Toulouse). Our data are compared to band structure calculations which were performed using the WIEN2K package [19].

Figure 1(a) shows raw magnetotorque $\tau(H)$ data for three values of x measured up to 55 T at $T \simeq 1.5$ K, with the magnetic field direction close to the c axis. The torque response for the higher T_c samples ($x = 0.33$, $T_c \simeq 30$ K and $x = 0.41$, $T_c \simeq 25$ K) is highly hysteretic. The irreversibility field $\mu_0 H_{\rm irr}$ increases substantially with x reaching a maximum of 51.5 T for the highest T_c sample ($x = 0.33$), which is close to the estimated H_{c2} value [17]. By subtracting a smooth polynomial background the oscillatory dHvA signal is clearly seen above $H_{\rm irr}$ [Fig. 1(b)] for all samples except for that with the highest T_c ($x = 0.33$).

Band structure calculations [20] of the Fermi surface of the end members of the $BaFe_2(As_{1-x}P_x)_2$ series are shown in Fig. 2. The two electron sheets at the zone corner are quite similar in size and shape in both compounds but there are significant differences between the hole sheets. In $BaFe_2As_2$ three concentric quasi-two-dimensional hole tubes are located at the zone center, whereas in $BaFe_2P_2$ the inner one of these tubes is absent whereas the outer tube has become extremely warped. The Fermi surface of $BaFe_2P_2$ is very similar to that for $SrFe_2P_2$ [12].

From the fast Fourier transform (FFT) spectra of the oscillatory data [Fig. 1(c)] we can extract the dHvA frequencies F. These are related to the extremal cross-sectional areas, A_k, of the Fermi surface orbits giving rise to the oscillations via the Onsager relation, $F = (\hbar/2\pi e)A_k$. The evolution of these frequencies (see Fig. 2) as the magnetic field is rotated from $B \parallel c$ axis ($\theta = 0°$) towards $B \perp c$ ($\theta = 90°$), shows clearly that they originate from quasi-two-dimensional Fermi surface sheets ($F \sim 1/\cos(\theta)$) as expected from the band structure.

For the following reasons, is very likely that the strong dHvA signals we see for $BaFe_2(As_{1-x}P_x)_2$ are from the electron sheets. In the other iron-phosphides: LaFePO [14], $CaFe_2P_2$ [13] and most importantly $SrFe_2P_2$ [12], the scattering rate on the electron sheets is always much lower than on the hole sheets and so these sheets give the strongest dHvA signals. Given the similarity in crystal structure and Fermi surface, particularly with $SrFe_2P_2$, this is also likely to be the case here. Comparing the dHvA data for $BaFe_2(As_{1-x}P_x)_2$ with the calculated dHvA frequencies for $BaFe_2P_2$ [Fig. 2(a)] we see that the splitting of the principal dHvA peaks coming from the c axis dispersion (minimal and maximal areas) is in good agreement with the calculation for the electron sheets. This is most clearly demonstrated for $x = 0.71$ [compare Figs. 2(a) and 2(c)]. The band shifts needed to bring the calculated electron sheet frequencies into agreement with the data 45–75 meV are quite comparable to those for $SrFe_2P_2$ (50–60 meV). Finally, we note that the experimental values of the Hall coefficient [16] for these crystals are always negative, which again suggests that the electron sheets have the longest mean free path. Although there are other weak peaks in the FFT which could come from the hole sheets, further data measurements with improved signal to noise ratio are needed to confirm these.

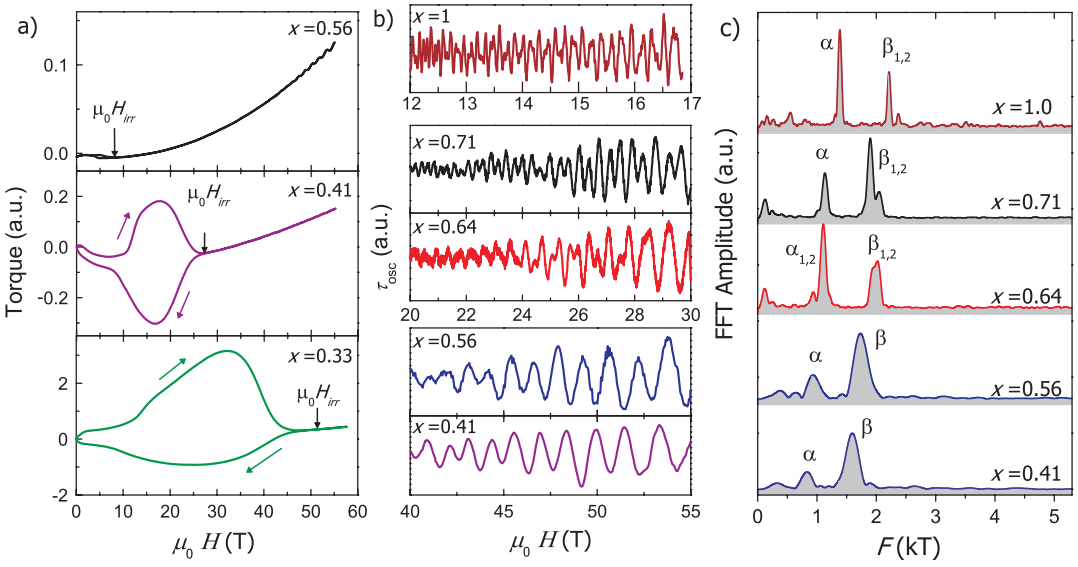

FIG. 1 (color online). (a) Raw torque data for $BaFe_2(As_{1-x}P_x)_2$ with $x = 0.33, 0.41, 0.56$ measured at 1.5 K. (b) The oscillatory part of torque for selected samples and (c) the corresponding Fourier transform for $x = 0.41, 0.56$ between 35–55 T at 1.5 K and $x = 0.64, 0.71$ between 20–30 T at 0.35 K as well as $x = 1$ between 12–16.8 T at 0.092 K.

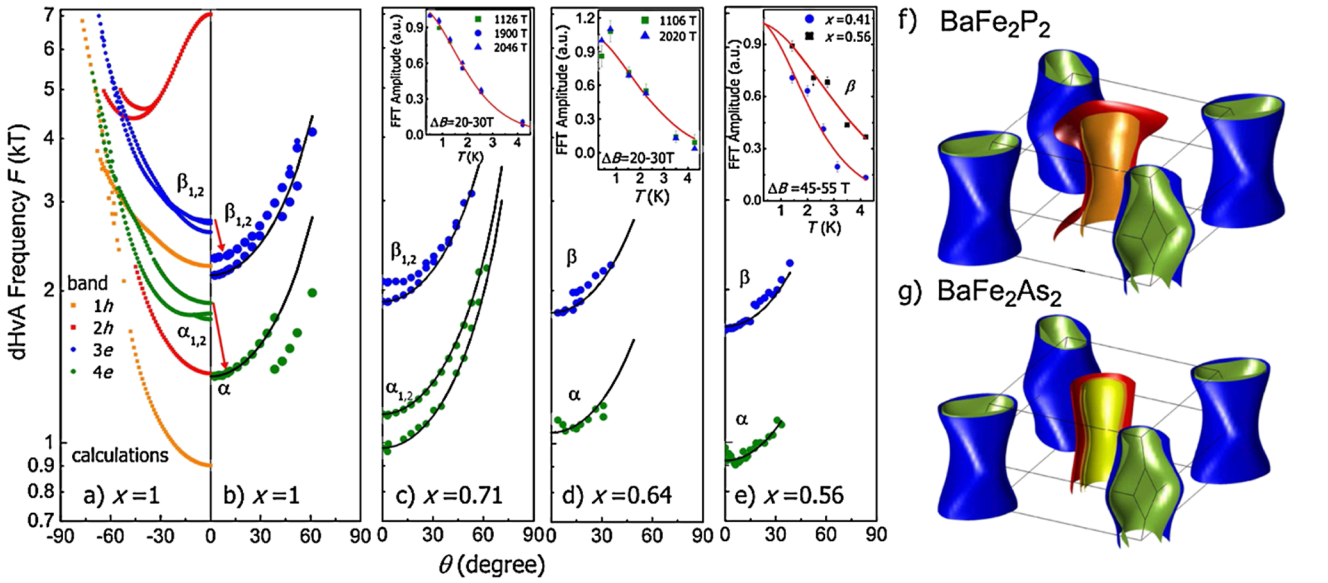

FIG. 2 (color online). (a) Angle dependence of the predicted orbits from $B \parallel [001]$ ($\theta = 0°$) to $B \parallel [100]$ ($\theta = 90°$) for $x = 1$ ($BaFe_2P_2$) and the electron orbits observed experimentally for (b) $x = 1$, (c) $x = 0.72$, (d) $x = 0.64$, (e) $x = 0.56$. Solid lines correspond to $F(\theta = 0)/\cos\theta$. The insets show the temperature dependence of the Fourier amplitudes for each composition, which are fitted (solid line) to the Lifshitz-Kosevich formula $X/\sinh X$, $X = 14.69 m^* T/B$ to determine the effective masses, m^* [23]. The calculated Fermi surfaces of the end members, (f) $BaFe_2P_2$ and (g) $BaFe_2As_2$ (nonmagnetic) are also shown.

As the sample composition is varied towards optimal doping, the dHvA signal is reduced but the oscillations from both electron sheets are clearly visible over the full doping range in sufficiently high fields [see Fig. 1(c)] [21]. Importantly, we observe that the frequency of both these electron orbits decreases linearly with decreasing x [see Fig. 3(a)]. As x decreases from 1 to 0.41 the Fermi surface cross-sectional area shrinks by $37 \pm 4\%$ and $30 \pm 4\%$ for the α and β frequencies respectively [22]. Although we do not clearly observe them, charge neutrality means that the hole sheets must shrink by the same factor.

The effective masses of the quasiparticles were determined by fitting the temperature dependent amplitude of the dHvA oscillations to the Lifshitz-Kosevich formula [23] (see insets of Fig. 2). As shown in Fig. 3(b), the effective mass increases significantly as x approaches the spin density wave ordered phase. At the same time T_c increases and shows a maximum at the boundary of the magnetic order. As no such mass increase is expected from the band structure (see below) the result implies a significant rise in the strength of the many-body interactions, most likely caused by spin-fluctuations. A similar striking rise in the mass enhancement close to an antiferromagnetic quantum critical point has also been observed in quasi-two-dimensional heavy-Fermion systems [24].

For $x = 1$ bare masses calculated from the band structure for the electron sheets vary from 0.8 to 1.0 m_e. To obtain a dHvA frequency of 1.55 kT, appropriate for $x = 0.41$, requires a rigid shift of the energy of band 4 [see Fig. 2(a)] by 170 meV. The bare mass then decreases from 0.92 to 0.81 m_e, in sharp contrast to the large rise seen in experiment. The many-body enhancement factor m^*/m_b therefore increases from ~ 2 to ~ 4 as x decreases from 1 to 0.41. Note that conventional electron-phonon coupling is weak in these materials, and is estimated to only account for $\sim 25\%$ of the observed mass enhancement [25].

To see whether these changes can be explained by conventional band structure effects we have approximated the band structure of $BaFe_2(As_{1-x}P_x)_2$ using the stoichiometric structure of $BaFe_2As_2$ or $BaFe_2P_2$ with the lattice constants and z fixed to the experimental values appropriate for the various values of x (which scale linearly with x [16]). We find that for both the As and P material the α and β frequencies vary relatively little with x. In Fig. 3(a) we show a weighted average of these calculated frequencies, $F_{av} = xF_P + (1 - x)F_{As}$ where F_P and F_{As} refer to the average of the maximal and minimal extremal frequencies calculated with the atom set to P or As, respectively. The calculated changes are much smaller than we observe experimentally, so it seems unlikely that the shrinking electron sheets can be explained by conventional band structure theory.

An alternative is that the shrinking is driven by many-body effects, for example, antiferromagnetic spin fluctuations which would be expected to grow strongly as the SDW state phase boundary is approached. As spin fluctuations with $\boldsymbol{Q} \simeq (\pi, \pi)$ scatter electrons from the electron to the hole sheets these can lead to a shrinking of both sheet volumes, accompanied by an increase in the quasiparticle mass renormalization [26,27] in agreement with our observations. If these same fluctuations are also responsible for the superconducting pairing it might be possible to use

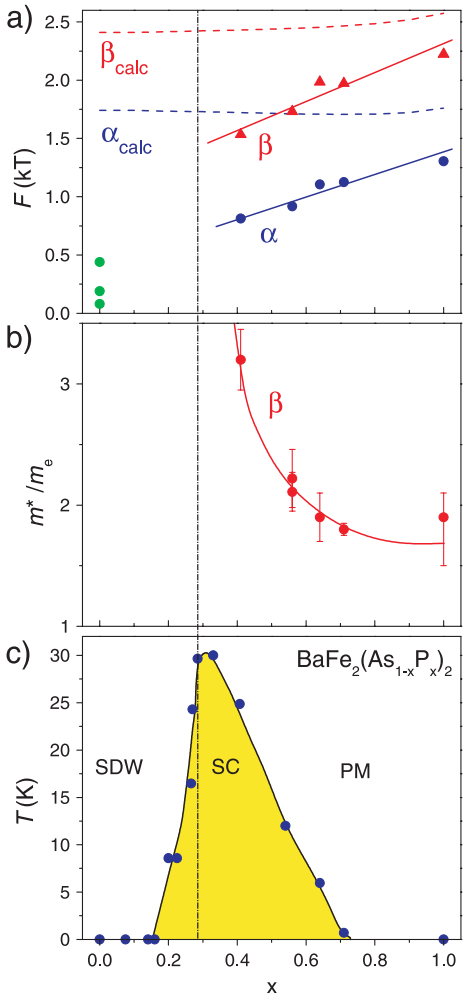

FIG. 3 (color online). (a) Experimental (solid symbols) average electron sheet frequencies (α and β) versus P content, x. The data for $x = 0$ are taken from Ref. [9]. The dashed lines show band structure predictions. (b) The variation with x of the quasiparticle effective masses, m^* and (c) T_c after Ref. [16]. The vertical dashed line marks the location of the onset of the appearance of magnetism at $T = 0$.

the measured band energy shifts and mass renormalizations as a way to measure the strength of the electron spin-fluctuation coupling and link this to T_c via Eliashberg theory. Indeed, just such a calculation was reported by Ortenzi *et al.* [26] for LaFePO. Using the band shifts needed to match the band structure calculations to dHvA experiments they were able to explain both measured mass renormalizations and T_c. If such quantitative agreement could be found using the present data for $BaFe_2(As_{1-x}P_x)_2$ this would provide strong evidence for spin-fluctuation mediated high T_c superconductivity in the iron pnictides.

We thank J. Analytis for helpful discussions and E. A. Yelland for the use of computer code. Part of this work has been done with the financial support of the UK's EPSRC and Royal Society, EuroMagNET under the EU contract no. 228043, Scientific Research on Priority Areas of New Materials Science Using Regulated Nano Spaces (20045008), Grant-in-Aid for Scientific Research on Innovative Areas "Heavy Electrons" (20102002), Specially Promoted Research (2001004) and Grant-in-Aid for GCOE program "The Next Generation of Physics, Spun from Universality and Emergence" from MEXT, Japan. Work performed at the NHMFL in Tallahassee, Florida, was supported by NSF Cooperative Agreement No. DMR-0654118, by the State of Florida, and by the DOE.

[1] M. Rotter, M. Tegel, and D. Johrendt, Phys. Rev. Lett. **101**, 107006 (2008).
[2] A. S. Sefat *et al.*, Phys. Rev. Lett. **101**, 117004 (2008).
[3] P. Alireza *et al.*, J. Phys. Condens. Matter **21**, 012208 (2009).
[4] S. Paulraj *et al.*, arXiv: 0902.2728.
[5] S. Jiang *et al.*, J. Phys. Condens. Matter **21**, 382203 (2009).
[6] I. I. Mazin, D. J. Singh, M. D. Johannes, and M. H. Du, Phys. Rev. Lett. **101**, 057003 (2008).
[7] K. Kuroki, H. Usui, S. Onari, R. Arita, and H. Aoki, Phys. Rev. B **79**, 224511 (2009).
[8] A. V. Chubukov, D. V. Efremov, and I. Eremin, Phys. Rev. B **78**, 134512 (2008).
[9] J. G. Analytis *et al.*, Phys. Rev. B **80**, 064507 (2009).
[10] N. Harrison *et al.*, J. Phys. Condens. Matter **21**, 322202 (2009).
[11] S. E. Sebastian *et al.*, J. Phys. Condens. Matter **20**, 422203 (2008).
[12] J. G. Analytis *et al.*, Phys. Rev. Lett. **103**, 076401 (2009).
[13] A. I. Coldea *et al.*, Phys. Rev. Lett. **103**, 026404 (2009).
[14] A. I. Coldea *et al.*, Phys. Rev. Lett. **101**, 216402 (2008).
[15] H. Sugawara *et al.*, J. Phys. Soc. Jpn. **77**, 113711 (2008).
[16] S. Kasahara *et al.*, arXiv:0905.4427.
[17] K. Hashimoto *et al.*, arXiv:0907.4399.
[18] Y. Nakai *et al.*, Phys. Rev. B **81**, 020503(R) (2010).
[19] P. Blaha, K. Schwarz, G. K. H. Madsen, D. Kvasnicka, and J. Luitz, *WIEN2K, An Augmented Plane Wave + Local Orbitals Program for Calculating Crystal Properties* (Karlheinz Schwarz, Techn. Universität Wien, Austria, 2001).
[20] Using the experimental atomic positions.
[21] The mean free path for the β orbits decreases from $\ell \sim$ 800 Å to 170 Å when x varies from $x = 1$ to 0.41.
[22] At the values of x where we can resolve a splitting of the dHvA peak due to c-axis dispersion we have plotted the average frequency.
[23] D. Schoenberg, *Magnetic Oscillations in Metals* (Cambridge University Press, London, 1984).
[24] H. Shishido, R. Settai, H. Harima, and Y. Onuki, J. Phys. Soc. Jpn. **74**, 1103 (2005).
[25] T. Yildirim, Phys. Rev. Lett. **102**, 037003 (2009).
[26] L. Ortenzi, E. Cappelluti, L. Benfatto, and L. Pietronero, Phys. Rev. Lett. **103**, 046404 (2009).
[27] H. Zhai, F. Wang, and D.-H. Lee, Phys. Rev. B **80**, 064517 (2009).